Molecular Biology of the Cell
Vol. 17, 1051–1064, March 2006

Conditional Dominant Mutations in the *Caenorhabditis elegans* Gene *act-2* Identify Cytoplasmic and Muscle Roles for a Redundant Actin Isoform[D] [V]

John H. Willis,* Edwin Munro,† Rebecca Lyczak,*‡ and Bruce Bowerman*

*Institute of Molecular Biology, University of Oregon, Eugene, OR 97403; and †Center for Cell Dynamics and Friday Harbor Laboratories, University of Washington, Friday Harbor, WA 98250

Submitted September 23, 2005; Revised December 30, 2005; Accepted January 4, 2006
Monitoring Editor: Sandra Schmid

Animal genomes each encode multiple highly conserved actin isoforms that polymerize to form the microfilament cytoskeleton. Previous studies of vertebrates and invertebrates have shown that many actin isoforms are restricted to either nonmuscle (cytoplasmic) functions, or to myofibril force generation in muscle cells. We have identified two temperature-sensitive and semidominant embryonic-lethal *Caenorhabditis elegans* mutants, each with a single mis-sense mutation in *act-2*, one of five *C. elegans* genes that encode actin isoforms. These mutations alter conserved and adjacent amino acids predicted to form part of the ATP binding pocket of actin. At the restrictive temperature, both mutations resulted in aberrant distributions of cortical microfilaments associated with abnormal and striking membrane ingressions and protrusions. In contrast to the defects caused by these dominant mis-sense mutations, an *act-2* deletion did not result in early embryonic cell division defects, suggesting that additional and redundant actin isoforms are involved. Accordingly, we found that two additional actin isoforms, *act-1* and *act-3*, were required redundantly with *act-2* for cytoplasmic function in early embryonic cells. The *act-1* and *-3* genes also have been implicated previously in muscle function. We found that an ACT-2::GFP reporter was expressed cytoplasmically in embryonic cells and also was incorporated into contractile filaments in adult muscle cells. Furthermore, one of the dominant *act-2* mutations resulted in uncoordinated adult movement. We conclude that redundant *C. elegans* actin isoforms function in both muscle and nonmuscle contractile processes.

INTRODUCTION

Actin is a highly conserved ATPase that assembles into cytoskeletal polymers called microfilaments. Both the hydrolysis of ATP to ADP, and the activities of actin-associated proteins, regulate microfilament assembly and disassembly, influencing microfilament dynamics and contractility (Sablin *et al.*, 2002). Microfilaments are required for many cellular processes including cell adhesion, cell migration, cell polarity, cytokinesis, endocytosis, muscle contraction, synapse function, and transcription. The regulated dynamic properties of microfilaments are important for many if not all of these roles.

The nonmuscle roles for microfilaments are often referred to as cytoplasmic, to distinguish them from the better understood contractile processes that occur in muscle cell myofibrils. These different functions appear to depend in part on the differential expression of closely related but distinct actin isoforms (Herman, 1993; Khaitlina, 2001). For example, vertebrate genomes encode several different actin isoforms, some specifically expressed in muscle and others in nonmuscle cell types. These different expression patterns correlate with limited differences in primary amino acid sequence. For example, the length and charge of the N-terminus varies among different isoform classes, and other amino acid positions also exhibit isoform-specific variations (Herman, 1993; Khaitlina, 2001). Functional studies indicate that the sequence differences used to classify actin isoforms are important. For example, the lethality associated with loss of a cardiac isoform in mice could not be rescued by cardiac expression of a smooth muscle isoform (Kumar *et al.*, 1997). In addition, overexpression of different human cytoplasmic actin isoforms in cell culture resulted in distinct cellular phenotypes (Schevzov *et al.*, 1992).

Invertebrate actin isoforms are less distinctive in amino acid sequence and in general more closely resemble vertebrate cytoplasmic actins (Khaitlina, 2001). Nevertheless, invertebrate isoforms also have been shown to have specific cytoplasmic or muscle functions. For example, the genome of the fruit fly *Drosophila melanogaster* encodes six actin isoforms. Two appear to function specifically as cytoplasmic actins, whereas two others are specifically expressed in larval muscle, and still two others in adult muscle (Fyrberg *et al.*, 1980, 1981). One adult-specific muscle isoform, Act-88F, is essential for flight. Flight was restored in mutants lacking Act-88F, when the Act-88F promoter was used to drive expression of the other adult muscle isoform. However, neither of the two larval muscle isoforms, nor one of the cytoplasmic isoforms, could restore flight when expressed using the Act-88F promoter (Fyrberg *et al.*, 1998). Similarly,

This article was published online ahead of print in *MBC in Press* (http://www.molbiolcell.org/cgi/doi/10.1091/mbc.E05–09–0886) on January 11, 2006.

[D] [V] The online version of this article contains supplemental material at *MBC Online* (http://www.molbiolcell.org).

‡ Present address: Biology Department, Ursinus College, Collegeville, PA 19426.

Address correspondence to: Bruce Bowerman (bbowerman@molbio.uoregon.edu).

Supplemental Material can be found at:
http://www.molbiolcell.org/content/suppl/2006/01/11/E05-09-0886.DC1

expression of the beta form of human cytoplasmic actin, driven by the Act-88F promoter, did not restore flight, even though it was incorporated into microfilaments (Brault *et al.*, 1999). Finally, one of the two cytoplasmic isoforms in *Drosophila*, *Act5C*, is essential, but viability was restored in mutants lacking Act5c when the other cytoplasmic isoform, *Act42A*, was expressed from the *Act5C* promoter (Wagner *et al.*, 2002). Thus the two cytoplasmic isoforms appear interchangeable, but proper transcriptional control by the promoter is required for viability. These studies indicate that the cytoplasmic and muscle isoforms have at least some distinct functions, whereas isoforms within each class are more interchangeable.

The five different actin isoforms in the nematode *Caenorhabditis elegans* have not been studied as extensively as those in *Drosophila*. Three actin genes, *act-1*, *-2*, and *-3*, reside in a cluster on one chromosome, whereas *act-4* and *act-5* are each on different chromosomes (Files *et al.*, 1983; Macqueen *et al.*, 2005). As in other organisms, these actin isoforms are highly conserved in amino acid sequence. ACT-1 and -3 are 100% identical. ACT-2 and -4 are both 99%, and ACT-5 93% identical to ACT-1 and -3. Dominant mutations identified in *act-1* and *-3* result in disorganized contractile filaments in body-wall muscle cells and an uncoordinated mutant phenotype (Landel *et al.*, 1984), and a GFP::*act-1* fusion is expressed in body wall muscle and incorporated into contractile filaments (Dixon and Roy, 2005). A semidominant mutant with pharyngeal muscle pumping defects, but no body-wall muscle defects, was shown to have mis-sense mutations in both *act-2* and *-3* (Avery, 1993). Thus, either *act-2* or *-3*, or both, function in pharyngeal muscle cells. Although no mutations have been identified in *act-4*, an *act-4* reporter gene was expressed in body-wall and other muscle cell types (Stone and Shaw, 1993). Although studies in *C. elegans* have identified actin genes that function in muscle, less is known about which isoforms are required for cytoplasmic functions. A recent study has shown that *act-5* encodes a cytoplasmic actin required for the assembly of intestinal microvilli (Macqueen *et al.*, 2005). However, it remains unclear which *C. elegans* actin isoforms are required for other cytoplasmic processes.

Here we report our identification of two conditionally semidominant and embryonic-lethal mutations in the *C. elegans act-2* gene. These mutations alter conserved amino acids in the predicted ATP binding pocket of actin and promote contractile instabilities and ectopic furrowing in early embryonic cells, implicating ACT-2 as a cytoplasmic actin. However, a recessive *act-2* deletion mutant is homozygous viable, and we present evidence that both *act-1* and *-3* function redundantly with *act-2* in early embryonic cells. Finally, we show that a GFP::*act-2* fusion is expressed cytoplasmically throughout early embryos and, later in development, in epidermal cells and body wall muscle. Moreover, one of the dominant *act-2* mutants exhibits uncoordinated adult movement. These results, together with previous studies implicating *act-1*, *-2*, and *-3* in muscle function, show that in *C. elegans* three actin isoforms function redundantly as both cytoplasmic and muscle actins.

MATERIALS AND METHODS

C. elegans *Strains and Culture*

All strains were cultured by standard methods (Brenner, 1974). Bristol (N2) was the standard wild-type strain used in this study. The following alleles were used: LGI: *dpy-5(e61)*; LGII: *rol-6(e187)*; LGIII: *unc-32(e189)*; LGIV: *unc-5(e53)*; *him-8(e1489)*; LGV: *dpy-11(e224)*, *act-2(or295*SD,ts*)*, *act-2(or621*SD,ts*)*, *act-2(ok1229)*, *act-3(st22*d*)*, *unc-42(e270)*, *sma-1(e30)*, *egl-3(n150ts)*, *stDf4*; and LGX: *lin-2(e1309)*, *lon-2(e678)*. Conditional mutants were maintained by growth at the permissive temperature of 15°C. To obtain mutant embryos for phenotypic analysis, mutant L4 larvae were shifted to 26°C and grown to adulthood overnight, or young adults were grown at 26°C for at least 8 h. To assay the motility of wild-type and *act-2* mutant worms, L1 larvae produced at the permissive temperature of 15°C were shifted to the restrictive temperature until adulthood and then transferred to fresh plates for 6 h before recording images.

To determine if the *or295* and *or621* mutations were dominant or recessive, *or295/+* and *or621/+* L4 hermaphrodites raised at 15°C were shifted to 26°C and matured to adulthood overnight. Adults were transferred to fresh plates, allowed to lay eggs for several hours, and then removed. The fraction of embryos that hatched was scored 24 h after removal of the adults. In addition, *unc-42(e270) or295/+* hermaphrodites maintained at 15°C were shifted to 26°C as L4s and matured to adulthood overnight to produce broods of embryos. Twenty-two percent of the hatched embryos (n = 215) matured into Unc adults that were fertile and made dead embryos, indicating that the embryonic lethality observed in the broods of the *unc-42 or295/+* hermaphrodites was due to a maternal-effect dominance.

Positional Cloning of act-2(or295) and act-2(or621)

The *or295* and *or621* alleles were identified in screens for temperature-sensitive, embryonic-lethal mutations, using EMS and ENU mutagenesis, respectively, as described previously (Encalada *et al.*, 2000). The *or295* and *or621* mutations were backcrossed to the wild-type N2 strain eight and four times, respectively, in all strains used for phenotypic analysis.

Linkage group and 3-factor mapping were done as described previously (Brenner, 1974). Linkage group mapping was done using the strains MT3751 [*dpy-5(e61) I; rol-6(e187) II; unc-32(e189) III*], MT464 [*unc-5(e53) IV; dpy-11(e224) V; lon-2(e678) X*], EU1073 [*him-8(e1489) IV; act-2(e295) V*], and EU1296 [*him-8(e1489); act-2(or621) V*]. Both *or295* and *or621* mapped to LGV. Three-factor mapping with *act-2(or295*) was done using *dpy-11(e224) unc-76(e911) V* (map positions 0 and + 7.12), *unc-42(e270) sma-1(e30) V* (map positions +2.19 and +3.46), and *egl-3(n150ts) emo-1(oz1) sma-1(e30)* (map positions + 2.32, +2.83 and +3.46). Homozygous *emo-1(oz1*) worms are sterile. Using the *egl-3 emo-1 sma-1* chromosome in trans to *or295*, we found that in 53/53 Egl-non-Ste recombinants *egl-3* became linked to *or295*, whereas in 12/21 Sma-non-Ste recombinants, *sma-1* became linked to *or295*, placing *or295* at 3.0 map units. Three-factor mapping for *or621* was done using *dpy-11(e224) unc-76(e911)* in trans to *or621*. In 7/15 Dpy-non-Unc recombinants, *dpy-11* became linked to *or621*, whereas in 7/10 Unc-non-Dpy recombinants, *unc-76* became linked to *or621*, placing *or621* at roughly +2.85 map units on LGV. The cluster of *act-1*, *-2*, and *-3* is located to the right of *emo-1*, at about +3.0 map units, and *act-2* mRNA has been shown to be enriched in a germline cDNA library, suggesting it is maternally expressed (Piano *et al.*, 2000). We therefore sequenced the *act-1*, *-2*, and *-3* genes in genomic DNA from homozygous *or295* and homozygous *or621* worms. DNA fragments spanning each gene (from 100 base pairs 5′ of the predicted translational start site to 100 base pairs 3′ of the predicted stop codon) were amplified by PCR, and the products were isolated using a QIAquick Gel Extraction Kit (Qiagen, Chatsworth, CA). For each fragment, three pools of PCR products were independently isolated and combined for DNA sequencing reactions. DNA sequencing was done using the Beckman Quickstart Dye Terminator Kit and a Beckman CEQ8000 instrument, at the University of Oregon DNA Sequencing Facility. In *or295* genomic DNA, we identified a GGA to AGA mis-sense mutation at nucleotide number 46 in *act-2* that predicts a G15R amino acid change. In *or621* genomic DNA, we identified a TCC to GCC mis-sense mutation at nucleotide number 43 in *act-2* that predicts an S14A amino acid change. The amino acid numbers we use are based on the processed forms of actin, after the expected posttranslational removal of N-terminal residues. No nucleotide changes relative to wild type were detected in the *act-1* and *-3* genes in *or295* and *or621* genomic DNA. No nucleotide changes relative to wild type were detected in *act-2* after amplification from genomic DNA of the *lin-2(e1309) X* strain used as the background for the original isolation of *or295* and *or621*.

The *C. elegans* actin structure shown in Figure 3 was viewed using Cn3D version 4.1 from NCBI (http://www.ncbi.nlm.nih.gov). Files were exported as .png files and viewed by image J.

Single Oocyte RT-PCR and GFP::ACT-2 Translational Fusion Construction

Preparation of single oocytes for nested RT-PCR was performed as described (Rutledge *et al.*, 2001), but with the following changes. Isolated gonads were sheared through the glass needle of a mouth pipette to dislodge mature oocytes from the somatic gonad. Mature oocytes were transferred to watch glasses with fresh egg buffer twice before final transfer to a 0.65-ml Eppendorf tube containing 2 μl egg buffer. For RT-PCR we used the Invitrogen (Carlsbad, CA) SuperScript One-Step RT-PCR and followed the manufacturers protocol. The cDNA synthesis was carried out at 55°C for 30 min after DNase treatment. The first PCR reaction went for 15 cycles and 2 μl of this product was used for a second PCR reaction for an additional 25 cycles. Five microliters of each reaction was loaded per well. To determine that the PCR product was not amplified from genomic DNA, we used gene-specific PCR primers

that flanked the last intron (at least 45 bp in length) Samples were run on a 1.5% agarose gel and a 50- and a 100-base pair DNA ladder from New England Biolabs (Ipswich, MA) were used to determine size. Using these conditions, we could clearly distinguish between PCR products that differed by 45 base pairs. Furthermore, the primer pairs were designed to amplify differently sized RT-PCR products for each isoform, to distinguish each actin isoform. The conditions used did not allow us to compare isoform mRNA expression levels.

For construction of the GFP::*act-2* genomic transgene, we used PCR to amplify the *act-2* promoter region (starting 2.9 kb 5′ of the first codon) from the cosmid T04C12. The primers included a 5′ Not1 site and a 3′ Spe1 site for subcloning into pBluescript II KS+, using standard methods (Ausubel *et al.*, 1991). Subsequently, both a PCR-amplified GFP fragment (with primer-encoded 5′ and 3′ Spe1 sites), and the *act-2* exons and introns, plus 1 kb of 3′ genomic sequence (with primer-encoded 5′ Spe1 and a 3′ Kpn1 sites) were subcloned into the promoter vector. A linker encoding seven amino acids (G, S, S, T, R, G, A) was used between the 3′ end of the GFP and the start of ACT-2. Proper insert orientation and sequence fidelity were determined by DNA sequence analysis. To obtain a transgenic line that expresses the GFP::ACT-2 translational fusion, we injected N2 animals using standard methods (Mello *et al.*, 1991). The concentration of the injected GFP::*act-2* plasmid was 5 ng/μl, and the concentration of the dominant *rol-6* plasmid (pRF4) used as a transformation marker was 50 ng/μl. Genomic yeast DNA was used as carrier at a concentration of 50 ng/μl. One heritable extrachromosomal array was obtained in a transgenic strain that expressed GFP. We found that 33% of the progeny (n = 350) produced by transgenic animals inherited the array. Imaging of GFP expression in live embryos and anesthetized animals was done with a Bio-Rad 2100 Radiance confocal microscope (Richmond, CA), using a 60× oil immersion lens (use courtesy of Chris Doe, HHMI and the University of Oregon).

RNA Interference

Double-stranded RNA was prepared by amplifying the unique 3′UTR sequences of each actin gene with the following oligonucleotide pairs, using the indicated cosmids as templates: For *act-1* (T04C12): 5′ATGCACAACTTCGTCAACTTGCAC3′ and 5′TATCAATTTTTAAATTTTTATTCACAC3′; *act*-2 (T04C12): 5′ACGTTTTAACAATTTATGTAATAT3′ and 5′TAGAAATATTATTAAAATAAA3′; *act-3* (T04C12): 5′GCTCTTCGCCTTACCATTTTC3′ and 5′ATTCTGAAATTATTTATTGACTT3′; *act-4* (MO3F4): 5′ATTTTTTGCCCCTTCCACCC3′ and 5′GTCTTATTAAAAGCTTTATT3′; *act-5* (T25C8): 5′GCTGATTTTTTTTCAAATTTT3′ and 5′AAGTGGTCCTAACAAGTTT3′. PCR products were subcloned using the pGEM-t vector system (Promega, Madison, WI) and amplified with T7 and SP6 primers, with the SP6 primer including T7 sequences 5′ to the SP6 sequence. The amplified inserts were purified by phenol/chloroform extraction and ethanol precipitation (Ausubel *et al.*, 1991) and then used as templates for bidirectional transcription using T7 Polymerase (Promega). Double-stranded RNAs were microinjected into both arms of the gonad of young adult hermaphrodites using a Narishige micromanipulator. Injected *act-2(ok1229)* worms were incubated at 26°C; embryos were dissected from injected worms 12–16 h after injection. When we injected the same 3′UTR-specific dsRNAs into N2 animals, we observed fully penetrant embryonic/L1 larval lethality for the *act-1*, *-4*, and *-5* actin genes, whereas the only phenotype observed in the broods of *act-3 3′UTR*-injected animals was adult sterility (33%; n = 12). We observed no early embryonic cell division defects except after microinjection of *act-2 3′UTR* dsRNA into N2. However, as the *act-2(ok1229)* deletion allele is homozygous viable (Table 1), and microinjection of *act-2 3′UTR* dsRNA into *act-2(ok1229)* worms does not produce any lethality (Table 2), we suspect that the embryonic cell division defects observed after microinjection of *act-2 3′UTR* dsRNA into N2 worms is due either to short regions of high conservation with other actin genes or to spreading of the dsRNA into more highly conserved 5′ coding sequences (Alder *et al.*, 2003; May and Plasterk, 2005). Such spreading, if it occurred, appears to occur infrequently, as we did not observe any such effect for the other four 3′UTR dsRNA injections into N2 worms, and 3′UTR dsRNAs have also been used successfully to specifically deplete four different embryonic tubulin isoforms (Wright and Hunter, 2003; Phillips *et al.*, 2004). For depletion of *pfn-1*, *cyk-1*, and *mlc-4* gene products, exon fragments of at least 500 base pairs were amplified using PCR to generate DNA templates for the production of dsRNAs using T7 RNA polymerase (as described above).

Microscopy and Immunofluorescence

For time-lapse video microscopy, gravid hermaphrodites grown at the restrictive temperature of 26°C from the L4 stage were dissected in a watch glass filled with M9 buffer. Dissected embryos were transferred with a mouthpipette to a 3% agarose pad and covered with a 22 × 22-mm coverslip (Fisher Scientific, Pittsburgh, PA). DIC images were captured every 5 s using a Dage MT1 VE1000 digital camera and Scion Image software. For immunofluorescence staining of actin, tubulin, PGL-1, and PAR-2, we permeabilized embryos using a standard freeze-crack procedure (Bowerman *et al.*, 1992), plunging slides with coverslips into liquid nitrogen to freeze the samples, followed by removal of the coverslip and immersion of the slide for 15 min in methanol at −20°C. All rinses and antibody dilutions used phosphate-buffered saline (PBS). We blocked specimens before antibody staining with 1% BSA (PAR-2 and PGL-1 antibodies) or 3% BSA (actin and microtubules) for 30 min. We used the following antibodies: rabbit anti-PGL-1; 1:1000 (kindly provided by Dr. Susan Strome, Indiana University), rabbit anti-PAR-2; 1:15 (kindly provided by Dr. K. Kemphues, Cornell University), anti-TBB1 (kindly provided by Dr. P. Mains, University Calgary), and anti-actin (ICN Biochemicals, Costa Mesa, CA; 1 × 500 dilution in block). Primary antibodies were incubated at 4°C overnight in a humidity chamber. FITC-conjugated goat anti-mouse or anti-rabbit secondary antibodies (Jackson ImmunoResearch Laboratory, West Grove, PA) were used at 1:200 dilutions in PBS and incubated at room temperature for at least 1 h. DNA was labeled with 0.2 μM TOTO3 iodide (Molecular Probes, Eugene, OR). Specimens were sealed under coverslips using Slow Fade (Molecular Probes) and fingernail polish (Target, Eugene, OR). Fluorescent images were obtained using a Bio-Rad MRC 1024 laser scanning confocal microscope (Richmond, CA). For simultaneous staining of actin and tubulin we used identical laser settings and exposure times for all images (see Figure 7B).

For phalloidin staining of WT, *or295*, and *or621* embryos (see Figure 4), we raised embryos from each strain to L4 stage at 15°C and then transferred the worms to 26°C for 12–24 h. We then cut open the gravid adults in a drop of water to release eggs directly onto 1 × 5-inch glass slides with Teflon spacers (Cell line/Erie Scientific, Portsmouth, NH), coated with 1% poly-lysine, and exposed the eggs for 1 min to 1.5% sodium hypochlorite (Sigma, St. Louis, MO), and 250 mM KOH. We then rinsed the eggs briefly three times in egg salts (118 mM NaCl, 40 mM KCl, 3.4 mM CaCl, 3.4 mM MgCl, 5 mM HEPES, pH 7.2) and allowed them to recover in egg salts for 1 min. We then fixed embryos in 3% formaldehyde and 0.2% glutaraldehyde (Electron Microscopy Sciences, Hatsfield, PA), 0.1 mg/ml lysolecithin (Sigma), 60 mM Pipes, 25 mM HEPES, 10 mM EGTA, 2 mM $MgCl_2$, 100 mM dextrose for 15 min at room temperature (RT), rinsed them briefly three times in PBS with 0.1% Triton-X (PBT), and then stained them for 1 h at RT with Bodipy fl-phallicidin (Molecular Probes), at 1 U/200 μl in PBT. We then rinsed embryos three times for 5 min in PBS; we included DAPI at 0.1 μg/ml in the final rinse to stain DNA. We mounted embryos in 15 μl Fluoromount G (Southern Biotechnology, Birmingham, AL) under No. 1.5 glass coverslips and allowed the mountant to cure for >24 h before imaging the embryos. We collected all microfilaments images using a Bio-Rad Radiance 2000 confocal scanhead mounted on a Nikon E-800 upright scope. We used identical settings for all images. We then visualized DNA in the same embryo using a Delta Vision microscope (Applied Precision, Issaquah, WA).

RESULTS

Abnormal Membrane Ingressions and Protrusions in or295 and or621 Mutant Embryos

To identify genes required for microfilament-dependent processes during early embryogenesis in *C. elegans*, we screened chemically mutagenized nematodes for temperature-sensitive (ts) embryonic-lethal mutants. From a total of ~2300 such mutants, we found two (*or295* and *or621)* that exhibited abnormal membrane ingressions and protrusions in early embryonic cells (Figure 1A). Both *or295* and *or621* are partially conditional and semidominant. At the permissive temperature of 15°C, 62% (n = 240) of embryos produced by homozygous *or295* hermaphrodites (hereafter referred to as *or295* mutant embryos) failed to hatch. Similarly, 60% (n = 226) of *or621* mutant embryos produced at 15°C failed to hatch. At the restrictive temperature of 26°C, 98% (n = 467) of *or295* mutant embryos and 100% (n = 300) of *or621* mutant embryos failed to hatch (Table 1; see *Materials and Methods*). Furthermore, 12% (n = 300) of the embryos produced by heterozygous *or295/+* mothers at 26°C and 85% (n = 325) produced by *or621/+* mothers at 26°C failed to hatch (Table 1). Of the embryos from *or295/+* mothers that did hatch, 22% were *or295/or295* in genotype (see *Materials and Methods*). Thus the lethality observed in broods of heterozygous hermaphrodites was not restricted to homozygous mutant progeny but was caused by maternal expression of a dominant mutation, with *or621* being substantially more dominant than *or295*.

To examine early embryonic cell divisions, we used differential interference contrast (DIC) microscopy to make time-lapse video micrographs, after obtaining both mutant and wild-type embryos from worms raised at the restrictive

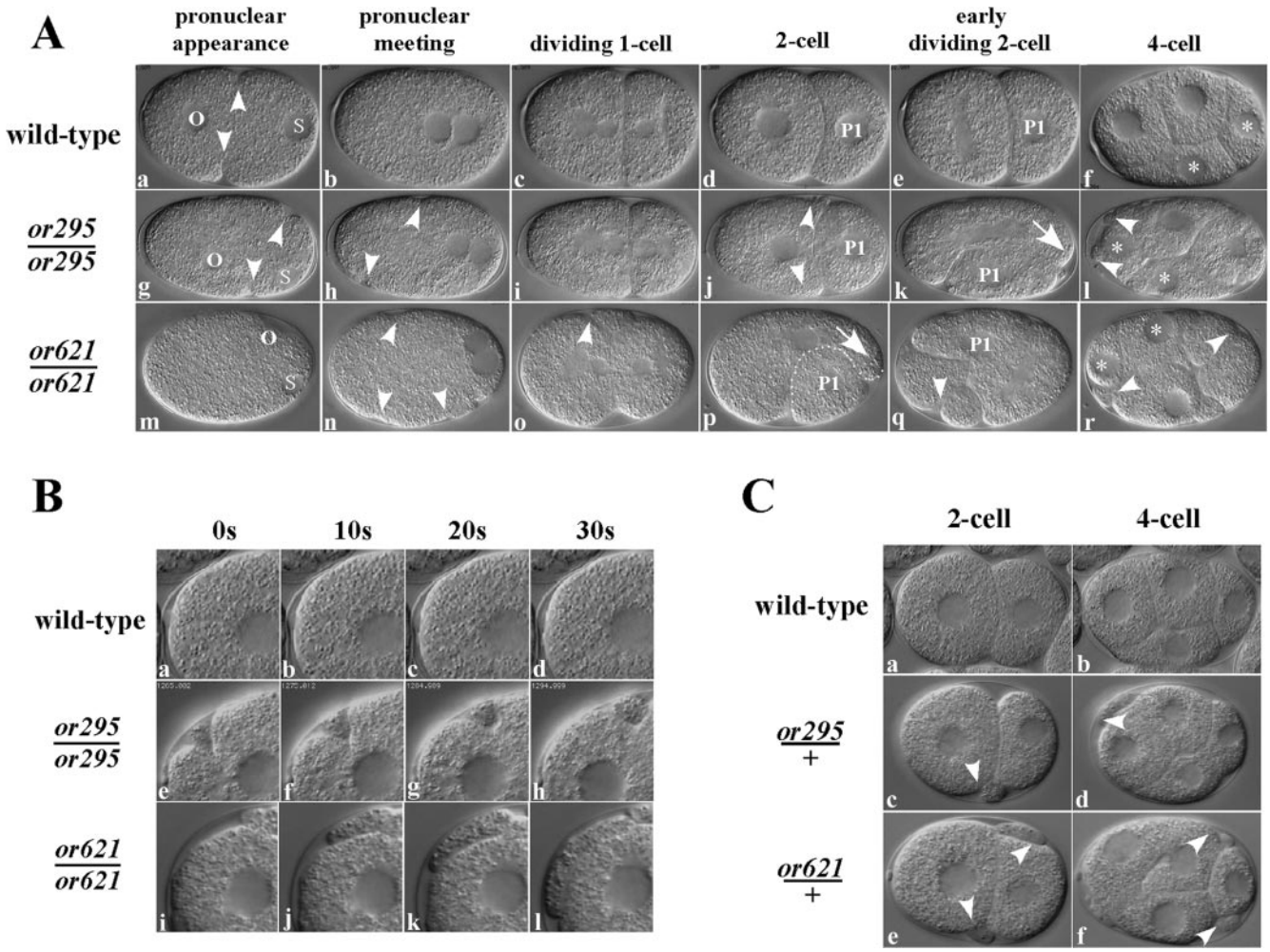

Figure 1. Ectopic membrane ingressions and protrusions in early *or295* and *or621* mutant embryos. (A) DIC micrographs from time-lapse images of live wild-type (a–f), *or295* (g–l) and *or621* (m–r) embryos. Arrowheads indicate the pseudocleavage furrow in a wild-type embryo, and abnormal membrane ingressions and protrusions in mutant embryos (a, g, h, j, l, n, o, q, and r). Oocyte (o) and sperm (s) pronuclei in 1-cell embryos are labeled; the posterior daughter of the first mitotic division (P_1) is labeled, and the two daughters of P_1 are indicated with asterisks. Arrows indicate the direction of cytoplasm protrusion in AB cells of *or295* and *or621* mutant embryos (k and p). Beginning at the 2-cell stage, these protrusions result in the mis-positioning of embryonic cells in *or295* and *or621* embryos. In some *or621* panels, not all nuclei are present in the focal plane shown (m). In this and all subsequent figures, anterior is to the left and posterior to the right. *C. elegans* embryos are ~50 μm in length. (B) Higher magnification DIC photomicrographs of the anterior cortex of the embryonic cell AB in live 2-cell stage wild-type, *or295,* and *or621* embryos. The membrane ingressions in mutant embryos often move along the surface of embryonic cells (*or295*; e–h), and the protrusions often grow in size over time (*or621*; i–l). Images were taken every 10 s from time-lapse video micrographs, beginning roughly at the completion of cytokinesis after the first mitotic division of each embryo. (C) Two- and 4-cell stage embryos produced by heterozygous *or295*/+ and *or621*/+ mothers raised at the restrictive temperature of 26°C often exhibit abnormal membrane ingressions and protrusions (arrowheads), due to the dominant nature of these mutations (see text for details; c-d and e-f).

temperature of 26°C (see *Materials and Methods*). The time-lapse sequences we made began shortly after the completion of meiosis, when the oocyte and sperm pronuclei become visible (Figure 1). In wild-type embryos, the initially diploid oocyte chromosome content is reduced to a haploid number by the extrusion of extra chromosomes into two polar bodies, followed by appearance of the oocyte pronucleus (Albertson, 1984). The first detectable defect we observed in mutant embryos was the presence of multiple maternal pronuclei before pronuclear migration and the first mitotic division, in 2 of 24 *or295* mutant embryos (8%) and in 4 of 21 *or621* mutant embryos (19%). We never observed this phenotype in wild-type embryos (n = 20). These results suggest that meiosis failed in some *or295* and *or621* mutant embryos, presumably due to defects in meiotic cytokinesis.

The most highly penetrant defects we observed in both mutants were abnormal ingressions and protrusions of the cell surface during interphase. In wild-type one-cell embryos, a prominent pseudocleavage furrow formed during pronuclear migration and then regressed after congression of the two pronuclei (Figure 1A, a and b). Anterior to the pseudocleavage furrow, the cell surface exhibited numerous shallow membrane ingressions, whereas posterior to the pseudocleavage furrow the surface remained largely quiescent (Figure 1A; Supplementary Movie 1). Before the first mitotic division in both *or295* and *or621* mutant embryos, we observed abnormal membrane ingressions and, in some cases, protrusions of the cell surface anterior to the pseudocleavage furrow during pronuclear migration in one-cell stage embryos (interphase and prophase of the first

Table 1. Embryonic lethality of *act-2* alleles and allelic combinations

Maternal genotype	% Emb. lethality (15°C)	% Emb. lethality (26°C)
N2	0 (385)	3 (478)
act-2(or295)/act-2(or295)	62 (240)	98 (467)
act-2(or295)/+	0 (210)	12 (360)
act-2(or621)/act-2(or621)	60 (226)	100 (300)
act-2(or621)/+	7 (415)	85 (325)
act-2(ok1229)/act-2(ok1229)	0 (345)	12 (515)
act-2(ok1229))/+	0 (196)	0 (288)
act-2(or295)/act-2(or621)	100 (230)	100 (270)
act-2(or295)/act-2(ok1229)	na	88 (420)
act-2(or295)/stDf4	na	100 (140)
act-2(or621)/act-2(ok1229)	na	97 (762)
act-2(or621)/stDf4)	na	100 (472)

Individually plated L4 animals were shifted to the indicated temperature for 24 h at which time the adult was removed. Twenty-four to 36 h later the plates were scored for embryonic lethality. *stDf4* is a small deficiency that has been shown to remove *act-2* and *-3*, but not *act-1*(Wormbase). na, not available.

mitotic cell cycle). These events were more dramatic and dynamic during interphase and prophase in 2- and 4-cell stage embryos (Figure 1, A and B; Supplementary Movies 1–5). Abnormal membrane ingressions were observed in all *or295* (n = 24) and *or621* (n = 21) mutant embryos. In contrast to the transient and shallow contractions observed in the anterior daughter of 2-cell stage wild-type embryos during early interphase, the deeper membrane ingressions in *or295* and *or621* mutant embryos persisted and often moved across the surface of embryonic cells, and the protrusions often grew in size (Figure 1B, e–h and i–l). These deeper membrane ingressions and the protrusions did not occur in wild-type embryos (Figure 1B, a–d). The abnormal membrane ingressions were more frequent in the anterior (AB) cell than in the posterior (P_1) cell in 2-cell stage mutant embryos. In *or295* mutants, we observed an average of 9.4 membrane ingressions during interphase in AB, whereas in P_1 we observed an average of 0.4 membrane ingressions (n = 10). In *or621* mutants, we observed an average of 3.8 ingressions in AB and 0.4 in P_1 (n = 10). This polarized distribution suggests that the anterior enrichment of actomyosin observed in wild-type embryos (Strome, 1986; Munro *et al.,* 2004) also occurred in these mutants. Finally, at the 2- and 4-cell stages in some *or295* mutant embryos, and more often in *or621* mutants, some membrane ingressions were associated with dramatic protrusions and cell migrations that disrupted the normal positions of early embryonic cells (Figure 1A, l and r; Supplementary Movies 3 and 5). We also observed abnormal membrane ingressions in embryos from heterozygous *or295*/+ and *or621*/+ mothers (Figure 1C, c-d, e-f; Supplementary Movies 6 and 7), consistent with the dominant nature of these two mutations (Table 1).

Because membrane ingressions in wild-type embryonic cells require the actomyosin cytoskeleton, we next asked if components and regulators of the cortical actomyosin cytoskeleton are required for the abnormal ingressions and protrusions observed in *or295* and *or621* mutant embryos. Previous work has shown that the cortical assembly of microfilaments in early embryonic cells requires a profilin called PFN-1 and a formin called CYK-1 (Severson *et al.,* 2002). Homologues of these two proteins have recently been shown to promote the barbed-end assembly of microfilaments in other organisms (Kovar *et al.,* 2005). Depletion of the myosin light chain MLC-4 or the nonmuscle myosin heavy chain NMY-2 does not impede the assembly or cortical enrichment of microfilaments, but these proteins are required for contractile force production in early embryonic cells (Guo and Kemphues, 1996; Shelton *et al.,* 1999). We used RNA interference (RNAi) to deplete, in *or295* and in *or621* mutant embryos, PFN-1 (n = 5 for *or295*, n = 4 for *or621*), CYK-1 (n = 4 for *or295*; n = 5 for *or621*), or MLC-4 (n = 6 for *or295*, n = 7 for *or621*; see *Materials and Methods*). In each case, as previously shown for the normal membrane ingressions in wild-type embryos (Shelton *et al.,* 1999; Severson *et al.,* 2002), the abnormal ingressions and protrusions were nearly or completely eliminated, as were other microfilaments-dependent processes, including cytokinesis (Figure 2; see Supplementary Movies 8–13). We conclude that the membrane ingressions observed in *or295* and *or621* mutant embryos result from and require actomyosin-dependent contractile forces.

Although the abnormal membrane ingressions in *or295* and *or621* mutant embryos appear to involve abnormal cortical actomyosin function, we did not detect any failure of cytokinesis in time-lapse videomicrographs of the first mitotic division or the divisions of AB and P_1 at the two-cell stage (n = 18 for *or295*; n = 15 for *or621*). As noted above, most of the abnormal membrane ingressions and protrusions occurred during interphase and early mitosis. During cytokinesis, ectopic furrows and protrusions were reduced in number and size (Supplementary Movies 2–5). These observations suggest that cortical actomyosin function in these mutant embryos was relatively normal during mitotic cytokinesis.

To characterize mitotic cytokinesis in more detail, we examined the timing of furrow initiation and the time required for completion of furrowing, during the first cell division in *or295*, *or621* and wild-type embryos, using DIC time-lapse videomicroscopy. We first measured the duration of mitosis, using nuclear envelope breakdown (NEB) and nuclear envelope reformation (NER) as rough markers for the beginning and end of mitosis. In dividing one-cell stage embryos, the duration of mitosis for *or295* and *or621* mutants was on average 1.3 and 1.5 times longer than normal: wild type = 5.8 min (n = 8); *or295* = 7.3 min (n = 10); *or621* = 8.6 min (n = 10). We next asked if this delay was restricted to either the time between NEB and cytokinesis furrow initiation or the time from cytokinesis furrow initiation to NER. We defined the initiation of cytokinesis as the first appearance of a detectable cleavage furrow that progressed with-

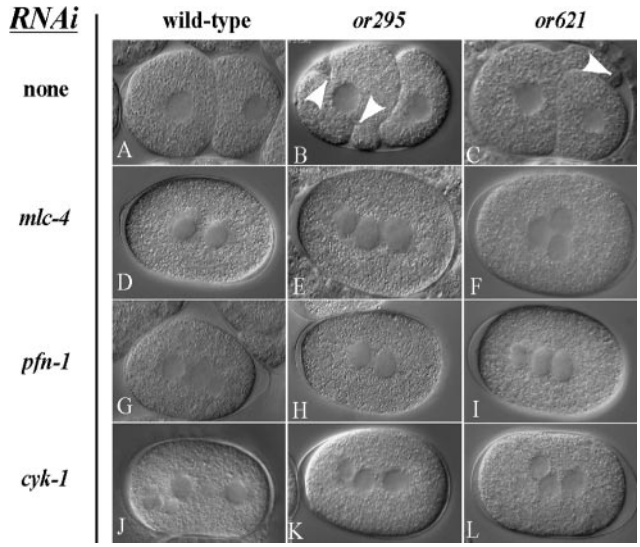

Figure 2. Ectopic membrane ingressions and protrusions in dominant *act-2* mutant embryos require a functional microfilament cytoskeleton. DIC photomicrographs of 2-cell stage wild-type, *or295,* and *or621* embryos (A–C) and equivalent stage wild-type, *or295* and *or621* embryos after RNAi-mediated depletion of actomyosin function (D–L). Arrowheads indicate ectopic ingressions (B) and a protrusion (C) in the mutant embryos. Depletion of actomyosin function prevents cytokinesis in all embryos and eliminates, or nearly eliminates, abnormal membrane ingressions and protrusions in the mutant embryos (C–F). The presence of more than two nuclei in many of the RNAi-depleted embryos is due to failures of meiotic cytokinesis and consequent aneuploidy (unpublished data). Also see Supplementary Movies 8–13.

out regression toward the central spindle. We found that the average time between NEB and cytokinesis furrow initiation in *or295* and *or621* mutant embryos was, respectively, 1.5- and 1.6-fold longer than normal: wild-type = 2.8 min (n = 8); *or295* = 4.1 min (n = 10); *or621* = 4.5 min (n = 10). In contrast, the average time from the beginning of cytokinesis to NER for *or295* embryos was relatively normal: wild-type = 3.0 min (n = 8); *or295* = 3.2 min (n = 10). However, in *or621* mutant embryos this latter interval was also longer than normal (4.1 min, or 1.4-fold longer; n = 10). Modest spindle checkpoint-dependent delays in mitosis have been reported in *C. elegans* mutants with defective mitotic spindles in early embryonic cells (Encalada *et al.,* 2005). However, we have not detected obvious defects in mitotic chromosome segregation in *or295* and *or621* mutants (Figure 1, and unpublished data), and the timing of these events was determined using only those embryos in which meiosis appeared to occur normally (with only a single maternal pronucleus present). Thus the increased time required for mitosis may reflect delays in the initiation and duration of cytokinesis.

or295 and or621 Are Alleles of act-2

To determine the identity of the gene(s) mutated in *or295* and *or621* mutants, we first used genetic mapping to determine the chromosomal location of these mutations. We found that both *or295* and *or621* are positioned at about + 3.0 map units on chromosome V (see *Materials and Methods*). Three of the five *C. elegans* actin genes reside in a cluster at roughly this location: *act-1*/T04C12.4, *act-2*/T04C12.5, and *act-3*/T04C12.6 (Figure 3A). We therefore sequenced the *act-1, -2,* and *-3* genes from genomic DNA isolated from homozygous *or295* and *or621* mutant worms and amplified using PCR (*Materials and Methods*). We did not find any mutations in the coding sequences of either *act-1* or *-3*, but in both mutants we identified mis-sense mutations near the beginning of the *act-2* open reading frame: a glycine to arginine mutation at codon 15 in *or295,* and a serine to alanine mutation at codon 14 in *or621* (Figure 3, B and C). Consistent with both mutations affecting *act-2* function, we also found that *or295* and *or621* failed to complement each other at the permissive temperature: none of the embryos produced at 15°C by *or295/or621* mothers hatched, whereas nearly all embryos produced at 15°C by *or295/+* and *or621/+* mothers hatched (Table 1). We conclude that *or295* and *or621* are mutant alleles of the *C. elegans act-2* gene. Both mutations change amino acids in the ATP-binding pocket of actin, as extrapolated from the structure of *C. elegans* actin (Figure 3 legend; Figure 3, B and C; Vorobiev *et al.,* 2003). Identical

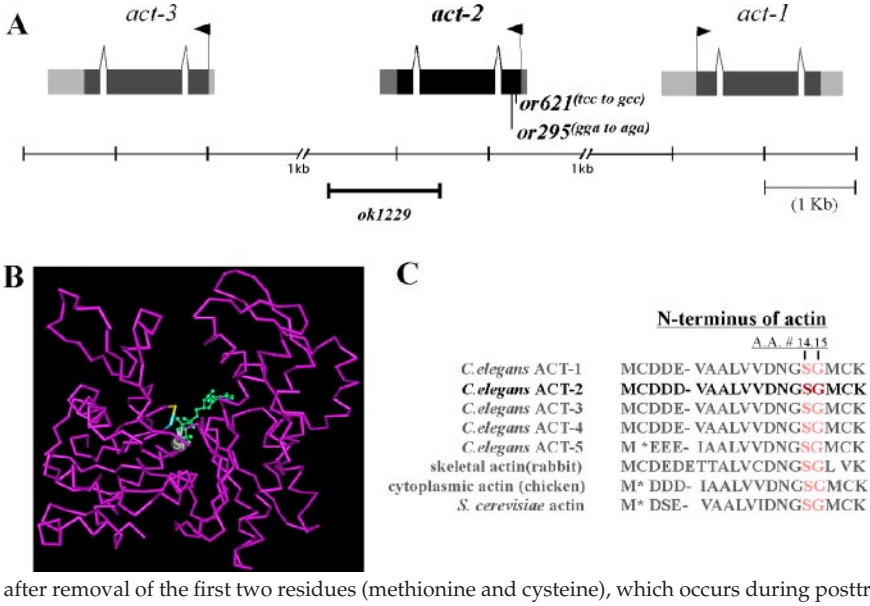

Figure 3. *or295* and *or621* are *act-2* alleles. (A) The actin gene cluster on linkage group V, where three of the five *C. elegans* actin genes reside, and the approximate location of the *act-2 (ok1229)* deletion and the *act-2(or295)* and *act-2(or621)* molecular lesions. (B) The *act-2(or295)* and *act-2(or621)* mutations alter conserved amino acids in a predicted loop that forms part of the ATP binding pocket of subdomain 1 of actin. The affected residues are highlighted in blue (S14A) and yellow (G15R) and are near the ATP molecule (green), which resides close to the center of the actin structure (purple). The structure, PDB name 1D4X, is from *C. elegans* Mg-ATP actin, purified from extracts and, thus, not isoform-specific (Vorobiev *et al.,* 2003; see *Materials and Methods*). (C) The N-terminal amino acid sequences (amino acids 1 through 19 or 20) of different actin isoforms in *C. elegans* and other eukaryotes. The residues in ACT-2 altered by the *or295* (G15R) and *or621* (S14A) mutations are highlighted in red. As is conventional for actin, numbers are assigned to amino acid residues after removal of the first two residues (methionine and cysteine), which occurs during posttranslational processing (adapted from Ono, 1999).

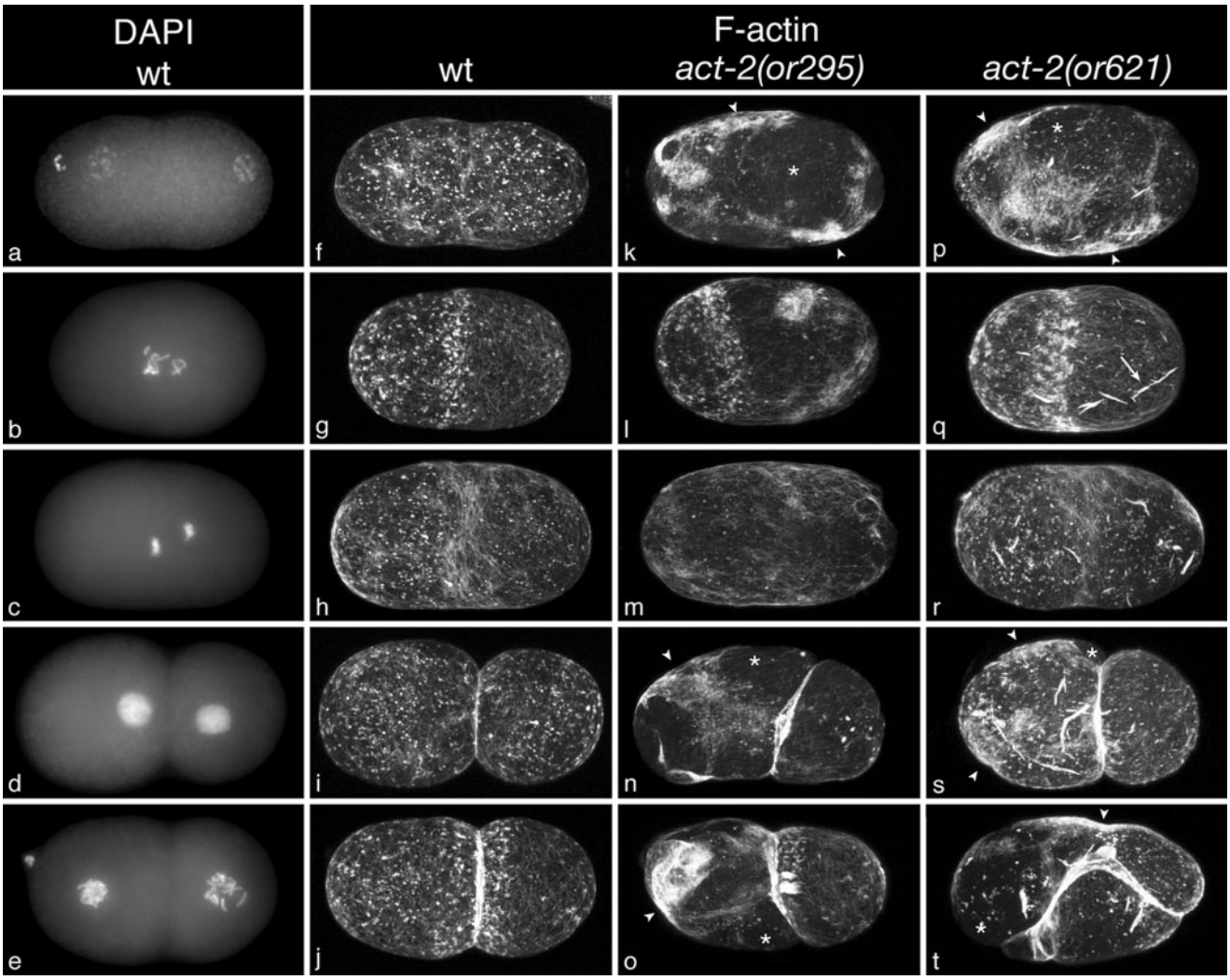

Figure 4. Cortical microfilaments during the first two embryonic cell cycles in fixed wild-type and dominant *act-2* mutant embryos. Wild-type embryos (a–j) costained with DAPI (a–e) to label DNA and Bodipy-fl-phallicidin (f–j) to label microfilaments. *act-2(or295*) embryos (k–o) and *act-2(or621*) embryos (p–t) also were stained with Bodipy-fl-phallicidin and DAPI. Embryos in each row are at the same point in the cell cycle, based on DAPI staining of chromosomes (not presented here for the mutant embryos). Each phallicidin-stained image is a maximum projection of 25 confocal sections taken at 0.25-μm intervals. All embryos were fixed and stained using the same procedures, imaged using the same confocal settings, and digitally processed identically. DAPI-stained images are maximum projections of 10–15 widefield epifluorescence images taken at 0.5-μm intervals. Both *or295* and *or621* embryos contain abnormally dense accumulations of cortical microfilaments (white arrowheads in k, n, o, p, s, and t). These are most pronounced within, but not restricted to, interphase embryos. Regions of dense accumulation often lie adjacent to regions that appear to be depleted of filaments relative to the wild type (white asterisks in k, n, o, p, s, and t), suggesting that microfilaments are abnormally distributed within the cortex. *act-2(or621)* embryos also accumulate dense microfilaments-containing structures (arrow in q), reminiscent of the barlike structures observed in yeast cells bearing the same point mutation (Chen and Rubenstein, 1995). These structures were mostly present deeper in the cytoplasm (unpublished data), but were also detected at or near the cortical surface. Late in anaphase, cortical microfilaments are reduced in density throughout the cortex outside the cleavage furrow, in both wild-type and mutant embryos (h, m, and r). The accumulation of microfilaments into a contractile ring late in anaphase was not obviously affected in the mutant embryos, although it is not apparent in this example of an *or295* mutant embryo (m).

actin mutations have been identified in other organisms (Chen and Rubenstein, 1995; Costa *et al.,* 2004).

Altered Distributions of Cytoplasmic Microfilaments in act-2(or295) and act-2(or621) Mutant Embryos

To investigate the effects of the dominant *act-2(or295*) and *act-2(or621*) mutations on microfilaments in early embryonic cells, we fixed wild-type and mutant embryos and examined the distribution and organization of microfilaments using fluorescently labeled phalloidin (*Materials and Methods*). As documented previously (Strome, 1986; Munro *et al.,* 2004), we observed focal accumulations of microfilaments in the cortex of early one-cell wild-type embryos (Figure 4F). These microfilament foci are associated with myosin-dependent contractions that drive cortical flow and membrane ingressions during polarization of the anterior-posterior body-axis in one-cell zygotes (Munro *et al.,* 2004). We also observed the previously documented anterior enrichment of cortical microfilaments that occurs before the first mitotic division in wild-type embryos (Figure 4G) and the subsequent enrichment of microfilaments in the contractile ring that occurs during cytokinesis (Strome, 1986; Munro *et al.,* 2004). In

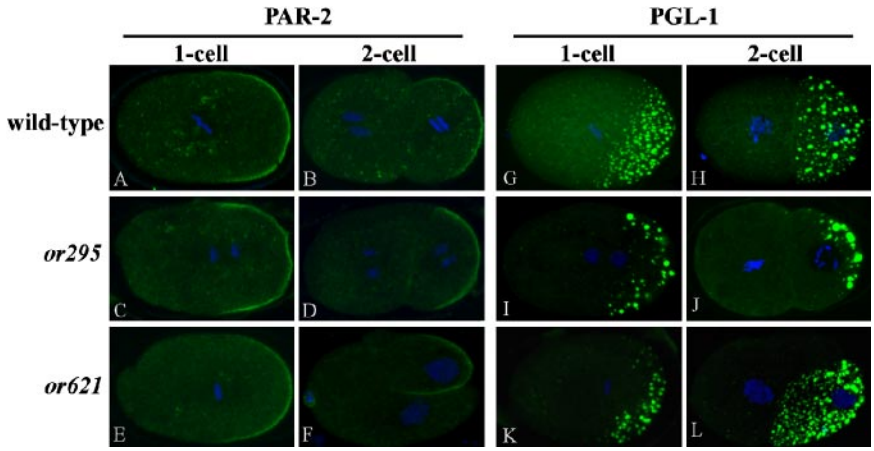

Figure 5. Anterior-posterior polarity appears normal in *act-2* mutant embryos. Fixed wild-type, *act-2(or295)*, and *act-2(or621)* embryos stained with fluorescently labeled antibodies that recognize the polarity regulatory protein PAR-2 (A–F) and the P granule component PGL-1 (G–L). Both proteins are localized normally in 1- and 2-cell stage *act-2(or295)* and *act-2(or621)* mutant embryos. Note that in F, even though the P_1 cell is becoming abnormally positioned, PAR-2 maintains a posterior cortical localization.

act-2(or295) and *act-2(or621)* mutant embryos, the general distribution of microfilaments throughout the first two mitotic cell cycles appeared relatively normal. Microfilaments were distributed throughout the cortex early in the one-cell stage (Figure 4, k and p), subsequently became enriched anteriorly as the zygote entered mitosis (Figure 4, l and q), and then concentrated in the cleavage furrow during cytokinesis (Figure 4, m–o and r–t). However, in both mutants we observed relatively large and dense patches of cortical microfilaments, particularly during interphase of the first and second cell cycles (Figure 4, k, n–p, and s), when actomyosin contractility is distributed evenly in small foci throughout the cortex in wild-type embryos (Munro *et al.*, 2004). Early in the first mitosis in the mutant embryos, we detected these more intensely staining patches within the microfilament-enriched anterior portion of the cortex and also within the posterior cortex (Figure 4, l and q), which is largely depleted of cortical microfilaments at this time in wild-type embryos (Figure 4g). We also observed increased levels of microfilaments between the cell boundaries in 2-cell stage mutant embryos (Figure 4, n, o, s, and t). Dense patches of microfilaments in 2-cell stage mutant embryos were more pronounced in the anterior AB cell than in the posterior P_1 cell, consistent with the greater number of cortical ingressions observed in AB in *act-2(or295)* and *act-2(or621)* mutant embryos (see above). Although the deep cortical ingressions observed in live mutant embryos were lost during the fixation process, we often observed shallow ingressions associated with dense patches of cortical microfilaments (arrowheads in Figure 4, n, o, s, and t).

Intriguingly, we also observed areas of the cortex with a pronounced depletion of microfilaments in *act-2(or295)* and *act-2(or621)* mutant embryos (Figure 4, k and p), in addition to the more restricted dense accumulations of microfilaments. Thus the denser accumulations may represent a redistribution of microfilaments within the plane of the cortex. As has been documented for wild-type embryos (Munro *et al.*, 2004), these increased microfilament densities likely correspond to foci of contractile NMY-2 associated with the ectopic membrane ingressions that we observed in live mutant embryos (Figures 1 and 2). Intriguingly, we also observed prominent, intensely staining barlike microfilaments structures in *act-2(or621)* embryos (Figure 4, q–t). Although we observed some barlike structures at the cortex (Figure 4, q–t), most were detected away from the cortex in the deeper cytoplasm (unpublished data).

Although we observed abnormal cortical microfilament distributions throughout most of the cell cycles in *or295* and *or621* mutant embryos, one exception occurred during anaphase. Ectopic accumulations of cortical microfilaments were nearly absent outside the cleavage furrow during anaphase in the mutant embryos (Figure 4, m and r). The absence of abnormal microfilament aggregations late in mitosis may explain why, in spite of the abnormal membrane ingressions that occurred throughout most of the cell cycle, we never observed cytokinesis failures during mitosis in *act-2(or295)* and *act-2(or621)* mutant embryos (see above).

Cell Polarity Appears Normal in act-2(or295) and act-2(or621) Mutant Embryos

Both time-lapse DIC videomicroscopy of live embryos (Figure 1) and the distribution of microfilaments in fixed embryos (Figure 4) suggest that the actomyosin-dependent establishment of anterior-posterior polarity at the one-cell stage (reviewed in Schneider and Bowerman, 2003) occurs normally in *act-2(or295)* and *act-2(or621)* mutant embryos. In time-lapse videomicrographs of mutant embryos ($n = 18$ for *or295*, $n = 16$ for *or621*), as in wild-type embryos, the pronuclei met near the posterior pole and moved to the center of the zygote before assembly of the first mitotic spindle (Figure 1; Supplementary Movies 1–5). By late anaphase, the first mitotic spindle was displaced posteriorly in all mutant embryos and the posterior daughter divided after the anterior daughter. Moreover, microfilaments in both mutants became enriched in the anterior portion of the embryo before the first mitotic division (Figure 4). These asymmetries also occur in wild-type embryos and indicate that anterior-posterior cell polarity in the one-cell zygote was not substantially affected by these dominant *act-2* mutations.

To test further for any defects in the establishment of an anterior-posterior body-axis, we examined the distribution of the cell polarity regulator PAR-2, which localizes to the posterior cortex in both the one-cell stage zygote and in P_1, the posterior daughter produced by the first mitotic division (Boyd *et al.*, 1996). We also examined the distribution of germline P granules, which are enriched in the posterior cytoplasm of the one-cell zygote and in P_1 (Kawasaki *et al.*, 1998). We stained fixed wild-type and mutant embryos with antibodies that recognize PAR-2 or antibodies that recognize the P granule component PGL-l (Boyd *et al.*, 1996; Kawasaki *et al.*, 1998). Both PAR-2 and P granules appeared to localize normally in *act-2(or295)* and *act-2(or621)* mutant embryos (Figure 5). We conclude that although the distribution and contractile properties of microfilaments are abnormal in *act-2(or295)* and *act-2(or621)* mutants, they nevertheless are competent for the establishment of anterior-posterior polarity.

Table 2. Embryonic lethality and embryonic cell division defects after depletion of different actin isoforms by 3′UTR-specific RNAi

Maternal genotype	% Embryonic lethality (15°C)	Early embryonic cell division defects
N2	0 (395)	No (n = 30)
act-2(ok1229)	0 (310)	No (n = 12)
act-1(3′UTR RNAi)	0 (175)	No (n = 10)
act-3(3′UTR RNAi)	0 (185)	No (n = 12)
act-1(3′UTR RNAi); act-2(ok1229)	100 (415)	Yes (n = 11)
act-3(3′UTR RNAi); act-2(ok1229)	100 (345)	Yes (n = 13)
act-1(3′UTR RNAi); act-3(3′UTR RNAi)	0 (196)	No (n = 8)
act-1(3′UTR RNAi); act-3(3′UTR RNAi);act-2(ok1229)	100 (230)	Yes (n = 14)
act-4(3′UTR RNAi); act-5(3′UTR RNAi);act2(ok1229)	0 (178)	No (n = 8)

Individually plated L4 animals were shifted to the indicated temperature for 24 h at which time the adult was removed. Twenty-four to 36 h later the plates were scored for embryonic lethality.

However, we have not examined the rate of polarization, and it remains possible that, as for cytokinesis, the dynamics of polarization were affected.

The act-2 Gene Is Not Required for Early Embryonic Cell Division

Although previous studies have shown that microfilaments are required for multiple processes during early embryogenesis (Hill and Strome, 1988, 1990), our identification of dominant mutations in *act-2* provides the first conclusive evidence for a specific *C. elegans* actin isoform being involved in cytoplasmic microfilament function in early embryonic cells. However, our analysis of these two mutants does not address whether *act-2* is required for early embryonic processes or whether other actin genes also contribute to embryonic actin pools. To examine the requirements for *act-2*, we obtained and analyzed a deletion allele, *act-2(ok1229)*, generated by the *C. elegans* knockout consortium (http://www.celeganskoconsortium.omrf.org). This deletion begins in the second exon, extends 705 base pairs beyond the *act-2* 3′UTR and removes 489/1131 base pairs of coding sequence (Figure 3A). Although *ok1229* appears to be a null allele, we did not detect any defects during the first mitotic division of the zygote in mutant embryos produced by homozygous *act-2(ok1229)* animals (n = 16). Indeed, all embryos produced at 15°C hatched, although 12% of the embryos produced by mothers raised at 26°C failed to hatch (Table 1). We conclude that *act-2* is not required for early embryonic cell divisions and probably functions redundantly with other actin genes at this stage.

act-1, -2, and -3 Function Redundantly in Early Embryonic Cells

To determine if other actin genes are required redundantly with *act-2* in the early embryo, we used RNAi to reduce the function of *act-1, -2, -3, -4,* and *-5* in *act-2(ok1229)* mutant worms. Because the coding sequences of the different actin genes are highly conserved and thus might cross-react if used for RNAi, we used the 3′UTR sequences, which range from 26 to 29% in nucleotide identity, to make dsRNA for microinjection into the ovaries of *act-2(ok1229)* worms (*Materials and Methods*). We then determined the percent embryonic lethality and made DIC time-lapse videomicrographs of individual embryos, 20–24 h after microinjection of dsRNAs. Microinjection of *act-2 3′UTR* dsRNA had no effect on embryonic viability in the *act-2(ok1229)* background (Table 2), which was expected as the deletion removes the 3′UTR. Furthermore, although microinjection of either *act-1* or *-3 3′UTR* dsRNAs into wild-type worms did not result in any early embryonic defects (unpublished data), microinjection of either *act-1* or *-3* 3′UTR dsRNA into *act-2(ok1229)* worms resulted in 100% embryonic lethality (Table 2) and in cytokinesis defects during early embryonic cell divisions (Figure 6, C and E). We observed more severe cytokinesis defects when *act-1* and *-3* 3′UTR dsRNAs were coinjected into *act-2(ok1229)* animals: cytokinesis was never successful, even at the second attempt (Table 2; Figure 6, D, F, and H). We did not detect any cytokinesis defects when *act-4* and *-5* 3′UTR dsRNAs were microinjected, separately or together, into *act-2(ok1229)* worms (Table 2, Figure 6, I and J). Nevertheless, microinjection of *act-4* and *-5* 3′UTR dsRNAs did result in highly penetrant embryonic or early larval lethality (Table 2), indicating that RNAi reduced gene function and presumably affected other processes later in development. We conclude that *act-1, -2,* and *-3* are required redundantly for microfilament-dependent processes in early embryonic cells, whereas *act-4* and *-5* probably make at most minor contributions to cytoplasmic microfilament function in early embryos.

To further examine the contributions of different actin genes, we used reverse transcriptase and PCR (RT-PCR) to detect specific actin isoform mRNAs, and immunolocalization to detect total actin protein. First, we isolated oocytes from wild-type and *act-2(ok1229*) mutant adults and then performed nested RT-PCR, using a 3′ primer complementary to the 3′UTR sequences specific for each actin gene and a 5′ primer corresponding to exon sequences 5′ of the last intron in each gene (*Materials and Methods*). We detected mRNA for all five actin genes in wild-type oocytes and mRNAs for each actin gene, except *act-2*, in oocytes from *act-2(ok1229)* worms (Figure 7A). In addition, we detected *act-2* transcripts in both *act-2(or295)* and *act-2(or621)* mutant embryos (Supplementary Figure 1), confirming that *act-2* transcripts are present in these dominant mutants. Finally, we used an anti-actin antibody to stain fixed embryos from wild-type and *act-2(ok1229)* worms and embryos from *act-2(ok1229)* worms 20–24 h after using microinjection of 3′UTR-specific dsRNAs to deplete both ACT-1 and -3. In wild-type and *act-2(ok1229)* embryos, we detected actin throughout the cortex of early embryonic cells (Figure 7B, a, c–e, g, and h). In contrast, we detected little or no cortical actin in embryos from *act-2(ok1229)* worms after microinjection of both *act-1* and *-3* dsRNAs (n = 15 embryos; Figure 7B, i, k, and l). These results are consistent with our functional analysis suggesting that *act-1, -2,* and *-3* are required redundantly for cytoplasmic microfilament function in the early *C. elegans* embryo.

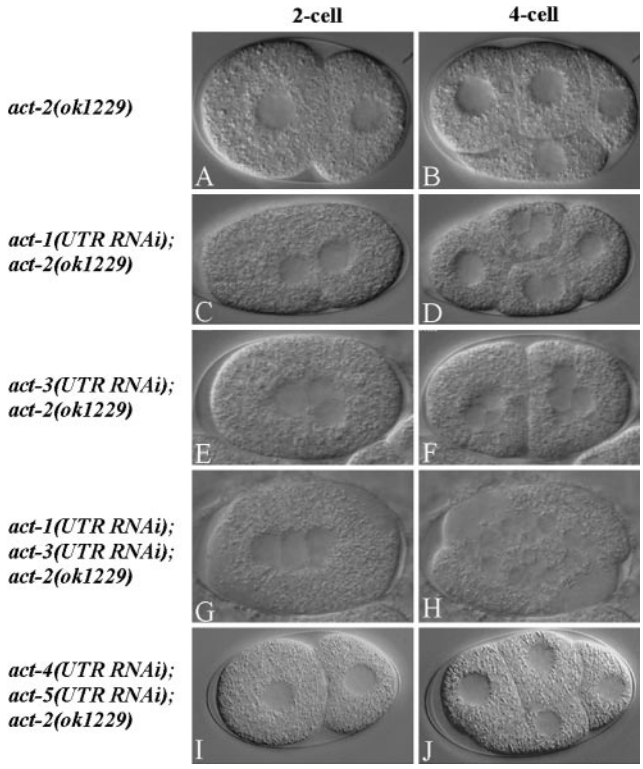

Figure 6. *act-1, -2,* and *-3* are redundantly required for early embryonic cell divisions. DIC photomicrographs of live 2- and 4-cell stage embryos from mothers homozygous for the *act-2(ok1229)* deletion (A and B) and equivalent stage embryos from *act-2(ok1229)* mothers after RNAi-mediated depletion of other actin isoforms, using 3′UTR dsRNA sequences specific for each isoform (see text and *Materials and Methods* for details). Early cell divisions appeared normal in embryos from *act-2(ok1229)* worms, although some embryonic lethality occurred in embryos produced at 26°C (Table 1). Depletion of either ACT-1 or -3 in the *act-2(ok1229)* background resulted in 100% embryonic lethality (Table 2) and in cytokinesis defects and thus multinucleate embryonic cells (C–F). Depletion of both ACT-1 and -3 in *act-2(ok1229)* embryos resulted in more severe cytokinesis defects (H). Depletion of both ACT-4 and -5 in *act-2(ok1229)* worms did not result in early cell division defects (I and J). See Table 2 for the number of embryonic cell divisions scored for cytokinesis defects. Also see Supplementary Movies 14–16.

ACT-2 Is Expressed and Required in Both Nonmuscle and Muscle Cell Types

Dominant mutations in *act-1* and *-3* have been shown previously to result in severe locomotion defects and abnormal muscle morphology, and the data we report here indicate that they also function cytoplasmically in early embryos. We therefore asked if *act-2* might also function in other cell types, including muscle cells, which previous reports have suggested (Avery, 1993). To address this possibility, we first constructed a GFP::ACT-2 translational fusion, using the endogenous *act-2* promoter, coding sequences, and 3′ region (*Materials and Methods*). We used this construct to generate a transgenic line that expresses GFP::ACT-2 from an extrachromosomal array (*Materials and Methods*). In embryos produced by transgenic hermaphrodites, we first detected GFP expression in embryos beginning at roughly the 20-cell stage (unpublished data), at the cortex, and throughout the cytoplasm of all embryonic cells (Figure 7C, panel A). Our failure to detect maternal expression in earlier stage embryos presumably was due to germline silencing of the extrachromosomal array, which often occurs with transgenes in *C. elegans* (Kelly and Fire, 1998). In addition to the cytoplasmic expression we observed throughout early embryonic cells, we also detected prominent GFP expression in the epidermis during elongation of the round embryo into a long, thin larva (Figure 7C, b). Actomyosin contractile forces are known to drive epidermal cell shape changes and elongation of the embryo in *C. elegans* (Priess and Hirsh, 1986). Thus it appears likely ACT-2 participates in this morphogenetic process, although our data do not conclusively demonstrate that GFP::ACT-2 colocalizes with endogenous actin in the circumferential actin bundles that mediate embryonic elongation. In adult animals, we reproducibly observed GFP expression in body wall muscle cells, incorporated into contractile filaments (Figure 7C, c), and in numerous neurons (unpublished data). To ask if ACT-2 functions in body wall muscle, we examined the motility of adult worms that were shifted as L1 larvae from the permissive temperature of 15°C to the restrictive temperature of 26°C until reaching adulthood (*Materials and Methods*). We observed locomotive defects in *act-2(or295*) mutant adults, but not in either wild-type worms or *act-2(or621)* mutants (Figure 7D; Supplementary Movies 14 and 15; unpublished data). We conclude that, like ACT-1 and -3, ACT-2 functions in both muscle and nonmuscle cell types.

DISCUSSION

The two conditional and dominant mutations we have identified in *C. elegans* ACT-2 alter conserved and adjacent amino acids that are predicted to form part of the ATP binding pocket. At the restrictive temperature of 26°C, these mutations result in similar but distinguishable defects, and in highly penetrant embryonic lethality. Although these dominant mutations implicate ACT-2 in early embryonic processes, a recessive deletion that removes a large portion of the *act-2* gene does not result in early embryonic cell division defects and causes only a weakly penetrant embryonic lethality. Consistent with this weak requirement for *act-2*, we have shown that *act-1* and *-3* are required redundantly with *act-2* for cytoplasmic microfilament function in early embryonic cells. As all three of these actin genes have been implicated in muscle function, our results indicate that multiple actin isoforms in *C. elegans* are required for actomyosin contractility in both nonmuscle and muscle cell types.

Actin Gene Redundancy in the Early C. elegans *Embryo*

Although the genomes of budding and fission yeast each have only a single, essential actin gene, multicellular eukaryotic organisms have multiple actin genes that encode identical or nearly identical isoforms. The *C. elegans* genome includes five actin genes. Two, *act-1* and *-3*, have identical open reading frame nucleotide sequences and reside in a cluster with *act-2*, which encodes an isoform 99% identical in amino acid sequence compared with the actin isoform encoded by its two neighbors. Similarly, ACT-4 exhibits 99% identity, whereas the ACT-5 amino acid sequence is the most divergent, with 93% identity compared with ACT-1 and -3 (Krause *et al.,* 1989; Macqueen *et al.,* 2005). Our identification of dominant mutations in *act-2* implicates this isoform in early embryonic cytoplasmic processes. Our use of 3′UTR-specific dsRNAs, to knock down by RNAi actin gene expression in a strain deleted for *act-2*, indicates that *act-1, -2,* and *-3* are required redundantly during early embryonic cell divisions. Consistent with this conclusion, we detected transcripts for the *act-1, -2,* and *-3* genes after using RT-PCR to amplify cDNAs from isolated oocytes. Although

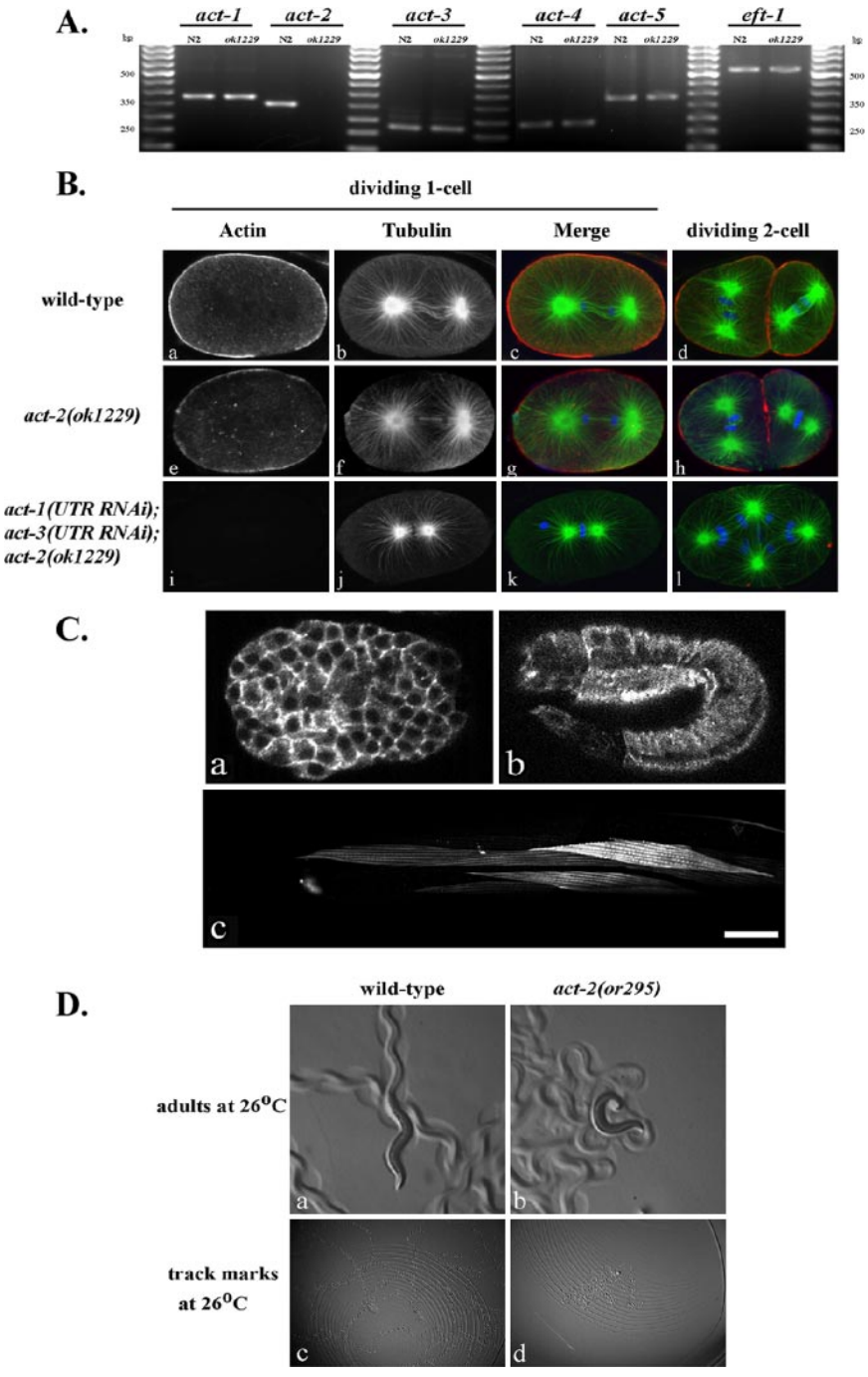

Figure 7. Actin gene expression in oocytes, early embryos, and adult muscle; motility defects in *act-2(or295)* adults. (A) Amplification of actin gene transcripts from isolated oocytes. Nested RT-PCR was performed using gene-specific 3′UTR primer sequences (see *Materials and Methods*). (B) Immunofluorescence photomicrographs of fixed wild-type and mutant embryos stained with fluorescently labeled antibodies that recognize actin (red) or tubulin (green); DNA (blue) was labeled with TOTO3. Confocal laser strength and antibody concentration were identical in all cases (see *Materials and Methods*). Little or no actin was detected in *act-1(3′UTR RNAi); act-3(3′UTR RNAi); act-2(ok1229)* embryos (i, k, and l). Extra chromosomes in panel k presumably are due to a failure in polar body extrusion during meiosis. (C) Cytoplasmic GFP::ACT-2 expression in live embryos was detected throughout the cytoplasm and at the cortex of all early embryonic cells (a), beginning at about the 20-cell stage (unpublished data), and in epidermal cells during embryonic elongation (b). GFP::ACT-2 also was detected in contractile filaments of adult striated muscle cells (c). Scale bar, 25 μm. (D) Motility defects in *act-2(or295)* adult animals at the restrictive temperature. Animals were placed on individual plates for 6 h before recording images, and track marks were recorded at 400× and 125× magnification, respectively. Also see Supplementary Movies 14 and 15, in which adult worm movements were recorded at 1 frame/s. Motility defects are apparent for *act-2(or295)*, whereas *act-2(or621)* mutants resemble wild-type adults in their motility.

we also detected both *act-4* and *-5* transcripts in isolated oocytes using RT-PCR, we did not detect any requirements for these two genes during early embryonic cell divisions. Although we cannot rule out early embryonic functions for *act-4* and *-5*, the use of 3′UTR-specific RNA to deplete these isoforms did result in highly penetrant embryonic and larval lethality, suggesting that RNAi effectively reduced the function of each gene. Furthermore, a recent study has shown that *act-5* is required only in cells with microvilli, and expression of ACT-1 driven by the *act-5* promoter cannot replace ACT-5 . Moreover, Macqueen *et al.* (2005) used an ACT-5-specific antibody to show that this isoform is expressed specifically only within cells that produce microvilli; no early embryonic expression was reported. We conclude that *act-1, -2,* and *-3* are required redundantly for cytoplasmic processes in the early embryo, whereas *act-4* and *-5* are less likely to be involved in these processes in spite of their maternal expression in oocytes.

Multiple C. elegans Actin Isoforms Are Required for Both Muscle and Nonmuscle Actomyosin Contractility

Our analysis of the redundant cytoplasmic requirements for three *C. elegans* actin genes is surprising because the same genes that we have shown are required for cell division in

the early embryo also are known to be involved in muscle contractile function. A previous analysis of *act-1, -2,* and *-3* suggested that these three isoforms are required redundantly for body wall muscle function (Landel *et al.,* 1984), and a mutant with mis-sense mutations in both *act-2* and *-3* has pharyngeal muscle pumping defects (Waterston *et al.,* 1984; Avery, 1993; Stone and Shaw, 1993). In addition, we have shown that a GFP::ACT-2 fusion protein driven by the *act-2* promoter is expressed cytoplasmically in multiple cell types and is incorporated into the contractile apparatus of adult muscle cells. Furthermore, adult *act-2(or295*) mutants shifted to the restrictive temperature exhibit defects in locomotion, consistent with ACT-2 functioning in body wall muscle cells. We conclude that in *C. elegans act-1, -2,* and *-3* are involved both in nonmuscle and muscle functions.

Our analysis *of C. elegans* actin isoform requirements contrasts sharply with several studies of actin isoforms in vertebrates and in *Drosophila*, which have shown that many actin isoforms are restricted in function to either muscle or nonmuscle roles (see *Introduction*). These restrictions have been suggested to reflect possible differences in microfilaments dynamics that depend on isoform composition, with muscle cell microfilaments being more stable than cytoplasmic microfilaments (Khaitlina, 2001). Our findings in *C. elegans* provide conclusive documentation that some actin isoforms can function in both cytoplasmic and muscle contractile processes. Consistent with these findings, *act-1, -2,* and *-3* encode amino acids at several positions that are conserved in cytoplasmic isoforms, and amino acids at other positions that are conserved in vertebrate muscle actin isoforms (unpublished data).

Although our results indicate that *act-1, -2,* and *-3* are required redundantly in the early embryo, the extent to which these three genes function in cytoplasmic processes later in development remains to be determined. Our findings that a GFP::ACT-2 translational fusion is expressed cytoplasmically throughout early stage embryos and in epidermal cells during morphogenetic processes later in development suggest that at least ACT-2 has additional cytoplasmic roles. However, the production of microvilli specifically requires ACT-5, which functions only in intestinal cells and a few other microvilli-containing cell types (Macqueen *et al.,* 2005). This requirement appears specific for ACT-5, as the engineered expression of ACT-1 within intestinal cells could not compensate for the loss of ACT-5 (Macqueen *et al.,* 2005). Thus at least this cytoplasmic role in *C. elegans* requires a distinct actin isoform. Similarly, a smooth muscle actin isoform cannot compensate for loss of a cardiac actin during mouse development (Kumar *et al.,* 1997), and a larval muscle actin isoform in *Drosophila* cannot compensate for loss of an adult muscle isoform (Fyrberg *et al.,* 1998). These results indicate that in some cases both cytoplasmic and muscle processes exhibit highly specific actin isoform requirements.

Dominant Mutations in act-2 Alter Conserved Amino Acids Previously Implicated in ATP Hydrolysis and Microfilament Dynamics

Both of the amino acids altered in the dominant *act-2* mutants that we identified have been implicated in ATP binding and hydrolysis, which play critical roles in actin structure, function, and dynamics (Sablin *et al.,* 2002; Vorobiev *et al.,* 2003). Crystallographic data, based on studies of actin from other organisms, suggest that six amino acids, including the two affected by the dominant mutations in *C. elegans act-2*, form hydrogen bonds with the γ- and β-phosphates of ATP, stabilizing the nucleotide-protein complex (Kabsch *et al.,* 1990; Kabsch and Vandekerckhove, 1992). These six amino acids are present in the actin subdomains 1 (Ser^{14}, Gly^{15}, Met^{16}, Leu^{16}) and 3 (Asp^{157}, Gly^{158}, Val^{159}). Five of these amino acids, including Ser^{14} and Gly^{15}, are conserved in all animal and plant actin isoforms and are thought to play critical roles in mediating the conformational changes associated with the hydrolysis of ATP to ADP (Sablin *et al.,* 2002).

An extensive mutational analysis of the sole actin in *S. cerevisiae* has shown that Ser^{14} in subdomain 1 is important for actin function both in vivo and in vitro (Chen *et al.,* 1995; Chen and Rubenstein, 1995; Schuler *et al.,* 1999). Budding yeast cells expressing S14A mutant actin displayed a temperature-sensitive lethality that is preceded by the disappearance of detectable actin cables and patches and the appearance of abnormal barlike structures (Chen and Rubenstein, 1995). In addition, in vitro studies of this mutant actin documented a 40–60-fold decrease in the affinity of actin for ATP and a decreased rate of ATP hydrolysis, in addition to an increased rate of polymerization and an altered susceptibility of microfilaments to protease treatment (Chen *et al.,* 1995; Chen and Rubenstein, 1995). Our analysis of the semidominant S14A *act-2(or621*) mutation in *C. elegans* revealed similarities to the corresponding mutation in yeast actin. These include a temperature-sensitive lethal phenotype and the appearance of abnormal barlike actin structures at the cortex and in the cytoplasm. The altered distribution of cortical microfilaments in *act-2(or621*) mutant embryos may reflect changes in actin dynamics consistent with the in vitro observations of a decreased rate of ATP hydrolysis and an increased rate of polymerization for yeast actin. In both the yeast and worm mutants, the accumulation of abnormal barlike microfilaments structures might reflect an alteration of microfilaments dynamics, with more stable microfilaments accumulating in dense aggregates and failing to recycle or redistribute more uniformly throughout the cortex.

A mutation identical to that in *act-2(or295*), G15R, has been reported in a human muscle actin called α-skeletal-muscle actin, or ACTA1. The corresponding ACTA1 mutation causes a dominant and lethal congenital myopathy in affected infants (Costa *et al.,* 2004). Expression of this mutant actin in cell culture produced aggregated microfilaments structures, suggesting it is incorporated into filaments but interferes with normal filament structure or dynamics (Costa *et al.,* 2004). Interestingly, we observed motility defects only in *act-2(or295)* animals, even though *act-2(or621)* results in a more highly penetrant and a more strongly dominant embryonic lethality. Moreover, *act-2(or621)* mutants exhibit more penetrant defects in meiosis, require more time to initiate and complete cytokinesis during mitosis, and undergo more prominent membrane protrusions. Thus the *act-2(or621)* S14A mutation more severely affects cytoplasmic processes, whereas only the *act-2(or295)* G15R mutation disrupts muscle function. Intriguingly, barlike MF aggregates in early embryonic cells are observed only in *act-2(or621)* mutants. Perhaps the *act-2(or621)* S14A mutation results in a more substantial stabilization of microfilaments and thereby disrupts cytoplasmic processes that require more dynamic microfilaments, without affecting the contractile properties in muscle cells that are thought to depend on more stable microfilaments (Khaitlina, 2001). To our knowledge, the effects of the *act-2(or295)* G15R mutation on actin properties and microfilaments dynamics in vitro have not been reported, making it more difficult to speculate on the consequences of this mutation. Nevertheless, one possibility is that the substitution of glycine with the much larger arginine in *act-2*(*or295)* disrupts the proper assembly or con-

formation of muscle actin myofibrils, independent of any effects on microfilament dynamics.

The dominant mutations we have identified in *C. elegans act-2* both lead to abnormal contractility and altered cortical microfilament distribution in early embryonic cells. As we did not detect an increase in actin levels in mutant embryo extracts (unpublished data), we speculate that these mutations either increase the rate of microfilament polymerization, or increase microfilament stability, and thereby disrupt the normal turnover and distribution of cortical microfilaments. Localized actomyosin-based contractions associated with anterior-posterior body-axis polarization in wild-type embryos appear to involve a limited form of contractile instability (Munro *et al.*, 2004). During axis polarization, focal contractions appear to be limited in size and duration by rapid actomyosin turnover within the foci (E. Munro, unpublished data). We speculate that the abnormal ingressions and protrusions we observe in *act-2(or295)* and *act-2(or621)* mutant embryos could involve an exaggerated form of the same contractile process, augmented by decreased microfilament turnover. In both mutants, the abnormal ingressions are associated with the accumulation of abnormally large and dense cortical microfilaments patches. Thus an important mechanism for the regulation of actomyosin contractility, particularly for cortical cytoplasmic function in nonmuscle cells, may be the modulation of microfilament polymerization or stability. Finally, it is interesting to note that the reduction in cortical microfilaments outside the cleavage furrow that occurs during late anaphase in wild-type embryos also occurs in *act-2(or295)* and *act-2(or621)* mutant embryos, despite their earlier accumulation of abnormally large and dense microfilament foci during interphase and early mitosis. This result suggests that a robust mechanism operates to down-regulate cortical microfilament stability outside the cleavage furrow during cytokinesis. The dominant mutations we have identified in *C. elegans act-2* may therefore provide useful genetic tools for identifying factors that modulate microfilaments dynamics during cell polarization and cell division.

ACKNOWLEDGMENTS

We thank Yuji Kohara for providing cDNA clones, the *C. elegans* Genetics Center, funded by the National Institutes of Health (NIH), and the *C. elegans* Gene Knockout Consortium, for providing strains. We are grateful to Chris Doe for use of the Bio-Rad Confocal microscope and Ken Kemphues and Susan Strome for the anti-PAR-2 and anti-PGL-1 antibodies. We thank Aaron Severson for initial characterization and genetic mapping of *or295*. We thank Julie Canman, Chris Doe, Morgan Goulding, Peter Rubenstein, and an anonymous reviewer for helpful comments on this manuscript. This work was supported by a NIH training grant (J.W.), by NIH Grant GM66050 (E.M.), and by NIH Grant R01GM58017 (B.B.).

REFERENCES

Albertson, D. G. (1984). Formation of the first cleavage spindle in nematode embryos. Dev. Biol. *101*, 61–72.

Alder, M. N., Dames, S., Gaudet, J., and Mango, S. E. (2003). Gene silencing in *Caenorhabditis elegans* by transitive RNA interference. RNA *9*, 25–32.

Ausubel, F. M., Brent, R., Kingston, R. E., Moore, D. D., Seidman, J. G., Smith, J. A., and Struhl, K. (1991). Current Protocols in Molecular Biology, New York: Greene Publishing Associates and Wiley-Interscience.

Avery, L. (1993). The genetics of feeding in *Caenorhabditis elegans*. Genetics *133*, 897–917.

Bowerman, B., Eaton, B. A., and Priess, J. R. (1992). skn-1, a maternally expressed gene required to specify the fate of ventral blastomeres in the early *C. elegans* embryo. Cell *68*, 1061–1075.

Boyd, L., Guo, S., Levitan, D., Stinchcomb, D. T., and Kemphues, K. J. (1996). PAR-2 is asymmetrically distributed and promotes association of P granules and PAR-1 with the cortex in *C. elegans* embryos. Development *122*, 3075–3084.

Brault, V., Reedy, M. C., Sauder, U., Kammerer, R. A., Aebi, U., and Schoenenberger, C. (1999). Substitution of flight muscle-specific actin by human (beta)-cytoplasmic actin in the indirect flight muscle of *Drosophila*. J. Cell Sci. *112* (Pt 21), 3627–3639.

Brenner, S. (1974). The genetics of *Caenorhabditis elegans*. Genetics *77*, 71–94.

Chen, X., Peng, J., Pedram, M., Swenson, C. A., and Rubenstein, P. A. (1995). The effect of the S14A mutation on the conformation and thermostability of *Saccharomyces cerevisiae* G-actin and its interaction with adenine nucleotides. J. Biol. Chem. *270*, 11415–11423.

Chen, X., and Rubenstein, P. A. (1995). A mutation in an ATP-binding loop of *Saccharomyces cerevisiae* actin (S14A) causes a temperature-sensitive phenotype in vivo and in vitro. J. Biol. Chem. *270*, 11406–11414.

Costa, C. F., Rommelaere, H., Waterschoot, D., Sethi, K. K., Nowak, K. J., Laing, N. G., Ampe, C., and Machesky, L. M. (2004). Myopathy mutations in alpha-skeletal-muscle actin cause a range of molecular defects. J. Cell Sci. *117*, 3367–3377.

Dixon, S. J., and Roy, P. J. (2005). Muscle arm development in *Caenorhabditis elegans*. Development *132*, 3079–3092.

Encalada, S. E., Martin, P. R., Phillips, J. B., Lyczak, R., Hamill, D. R., Swan, K. A., and Bowerman, B. (2000). DNA replication defects delay cell division and disrupt cell polarity in early *Caenorhabditis elegans* embryos. Dev. Biol. *228*, 225–238.

Encalada, S. E., Willis, J., Lyczak, R., and Bowerman, B. (2005). A spindle checkpoint functions during mitosis in the early *Caenorhabditis elegans* embryo. Mol. Biol. Cell *16*, 1056–1070.

Files, J. G., Carr, S., and Hirsh, D. (1983). Actin gene family of *Caenorhabditis elegans*. J. Mol. Biol. *164*, 355–375.

Fyrberg, E. A., Bond, B. J., Hershey, N. D., Mixter, K. S., and Davidson, N. (1981). The actin genes of *Drosophila*: protein coding regions are highly conserved but intron positions are not. Cell *24*, 107–116.

Fyrberg, E. A., Fyrberg, C. C., Biggs, J. R., Saville, D., Beall, C. J., and Ketchum, A. (1998). Functional nonequivalence of *Drosophila* actin isoforms. Biochem. Genet. *36*, 271–287.

Fyrberg, E. A., Kindle, K. L., and Davidson, N. (1980). The actin genes of *Drosophila*: a dispersed multigene family. Cell *19*, 365–378.

Guo, S., and Kemphues, K. J. (1996). A non-muscle myosin required for embryonic polarity in *Caenorhabditis elegans*. Nature *382*, 455–458.

Herman, I. M. (1993). Actin isoforms. Curr. Opin. Cell Biol. *5*, 48–55.

Hill, D. P., and Strome, S. (1988). An analysis of the role of microfilaments in the establishment and maintenance of asymmetry in *Caenorhabditis elegans* zygotes. Dev. Biol. *125*, 75–84.

Hill, D. P., and Strome, S. (1990). Brief cytochalasin-induced disruption of microfilaments during a critical interval in 1-cell *C. elegans* embryos alters the partitioning of developmental instructions to the 2-cell embryo. Development *108*, 159–172.

Kabsch, W., Mannherz, H. G., Suck, D., Pai, E. F., and Holmes, K. C. (1990). Atomic structure of the actin:DNase I complex. Nature *347*, 37–44.

Kabsch, W., and Vandekerckhove, J. (1992). Structure and function of actin. Annu. Rev. Biophys. Biomol. Struct. *21*, 49–76.

Kawasaki, I., Shim, Y. H., Kirchner, J., Kaminker, J., Wood, W. B., and Strome, S. (1998). PGL-1, a predicted RNA-binding component of germ granules, is essential for fertility in *C. elegans*. Cell *94*, 635–645.

Kelly, W. G., and Fire, A. (1998). Chromatin silencing and the maintenance of a functional germline in *Caenorhabditis elegans*. Development *125*, 2451–2456.

Khaitlina, S. Y. (2001). Functional specificity of actin isoforms. Int. Rev. Cytol. *202*, 35–98.

Kovar, D. R., Wu, J. Q., and Pollard, T. D. (2005). Profilin-mediated competition between capping protein and formin Cdc12p during cytokinesis in fission yeast. Mol. Biol. Cell *16*, 2313–2324.

Krause, M., Wild, M., Rosenzweig, B., and Hirsh, D. (1989). Wild-type and mutant actin genes in *Caenorhabditis elegans*. J. Mol. Biol. *208*, 381–392.

Kumar, A. *et al.* (1997). Rescue of cardiac alpha-actin-deficient mice by enteric smooth muscle gamma-actin. Proc. Natl. Acad. Sci. USA *94*, 4406–4411.

Landel, C. P., Krause, M., Waterston, R. H., and Hirsh, D. (1984). DNA rearrangements of the actin gene cluster in *Caenorhabditis elegans* accompany reversion of three muscle mutants. J. Mol. Biol. *180*, 497–513.

Macqueen, A. J., Baggett, J. J., Perumov, N., Bauer, R. A., Januszewski, T., Schriefer, L., and Waddle, J. A. (2005). ACT-5 is an essential *Caenorhabditis*

elegans actin required for intestinal microvilli formation. Mol. Biol. Cell *16*, 3247–3259.

May, R. C., and Plasterk, R. H. (2005). RNA interference spreading in *C. elegans*. Methods Enzymol. *392*, 308–315.

Mello, C. C., Kramer, J. M., Stinchcomb, D., and Ambros, V. (1991). Efficient gene transfer in *C. elegans*: extrachromosomal maintenance and integration of transforming sequences. EMBO J. *10*, 3959–3970.

Munro, E., Nance, J., and Priess, J. R. (2004). Cortical flows powered by asymmetrical contraction transport PAR proteins to establish and maintain anterior-posterior polarity in the early *C. elegans* embryo. Dev. Cell *7*, 413–424.

Ono, S. (1999). Purification and biochemical characterization of actin from *Caenorhabditis elegans*: its difference from rabbit muscle actin in the interaction with nematode ADF/cofilin. Cell Motil. Cytoskelet. *43*, 128–136.

Phillips, J. B., Lyczak, R., Ellis, G. C., and Bowerman, B. (2004). Roles for two partially redundant alpha-tubulins during mitosis in early *Caenorhabditis elegans* embryos. Cell Motil. Cytoskelet. *58*, 112–126.

Piano, F., Schetter, A. J., Mangone, M., Stein, L., and Kemphues, K. J. (2000). RNAi analysis of genes expressed in the ovary of *Caenorhabditis elegans*. Curr. Biol. *10*, 1619–1622.

Priess, J. R., and Hirsh, D. I. (1986). *Caenorhabditis elegans* morphogenesis: the role of the cytoskeleton in elongation of the embryo. Dev. Biol. *117*, 156–173.

Rutledge, E., Bianchi, L., Christensen, M., Boehmer, C., Morrison, R., Broslat, A., Beld, A. M., George, A. L., Greenstein, D., and Strange, K. (2001). CLH-3, a ClC-2 anion channel ortholog activated during meiotic maturation in *C. elegans* oocytes. Curr. Biol. *11*, 161–170.

Sablin, E. P., Dawson, J. F., VanLoock, M. S., Spudich, J. A., Egelman, E. H., and Fletterick, R. J. (2002). How does ATP hydrolysis control actin's associations? Proc. Natl. Acad. Sci. USA *99*, 10945–10947.

Schevzov, G., Lloyd, C., and Gunning, P. (1992). High level expression of transfected beta- and gamma-actin genes differentially impacts on myoblast cytoarchitecture. J. Cell Biol. *117*, 775–785.

Schneider, S. Q., and Bowerman, B. (2003). Cell polarity and the cytoskeleton in the *Caenorhabditis elegans* zygote. Ann. Rev. Genet. *37*, 221–249.

Schuler, H., Korenbaum, E., Schutt, C. E., Lindberg, U., and Karlsson, R. (1999). Mutational analysis of Ser14 and Asp157 in the nucleotide-binding site of beta-actin. Eur. J. Biochem. *265*, 210–220.

Severson, A. F., Baillie, D. L., and Bowerman, B. (2002). A formin homology protein and a profilin are required for cytokinesis and Arp2/3-independent assembly of cortical microfilaments in *C. elegans*. Curr. Biol. *12*, 2066–2075.

Shelton, C. A., Carter, J. C., Ellis, G. C., and Bowerman, B. (1999). The nonmuscle myosin regulatory light chain gene mlc-4 is required for cytokinesis, anterior-posterior polarity, and body morphology during *Caenorhabditis elegans* embryogenesis. J. Cell Biol. *146*, 439–451.

Stone, S., and Shaw, J. E. (1993). A *Caenorhabditis elegans* act-4:lacZ fusion: use as a transformation marker and analysis of tissue-specific expression. Gene *131*, 167–173.

Strome, S. (1986). Fluorescence visualization of the distribution of microfilaments in gonads and early embryos of the nematode *Caenorhabditis elegans*. J. Cell Biol. *103*, 2241–2252.

Vorobiev, S., Strokopytov, B., Drubin, D. G., Frieden, C., Ono, S., Condeelis, J., Rubenstein, P. A., and Almo, S. C. (2003). The structure of nonvertebrate actin: implications for the ATP hydrolytic mechanism. Proc. Natl. Acad. Sci. USA *100*, 5760–5765.

Wagner, C. R., Mahowald, A. P., and Miller, K. G. (2002). One of the two cytoplasmic actin isoforms in *Drosophila* is essential. Proc. Natl. Acad. Sci. USA *99*, 8037–8042.

Waterston, R. H., Hirsh, D., and Lane, T. R. (1984). Dominant mutations affecting muscle structure in *Caenorhabditis elegans* that map near the actin gene cluster. J. Mol. Biol. *180*, 473–496.

Wright, A. J., and Hunter, C. P. (2003). Mutations in a beta-tubulin disrupt spindle orientation and microtubule dynamics in the early *Caenorhabditis elegans* embryo. Mol. Biol. Cell *14*, 4512–4525.